Cancer Immunology Research

The Intratumoral Balance between Metabolic and Immunologic Gene Expression Is Associated with Anti–PD-1 Response in Patients with Renal Cell Carcinoma

Maria Libera Ascierto[1], Tracee L. McMiller[2], Alan E. Berger[3], Ludmila Danilova[1,4], Robert A. Anders[5], George J. Netto[1,5,6], Haiying Xu[7], Theresa S. Pritchard[2], Jinshui Fan[3], Chris Cheadle[3], Leslie Cope[1,4], Charles G. Drake[1,6], Drew M. Pardoll[1], Janis M. Taube[5,7], and Suzanne L. Topalian[2]

Abstract

Pretreatment tumor PD-L1 expression has been shown to correlate with response to anti–PD-1/PD-L1 therapies. Yet, most patients with PD-L1$^+$ tumors do not respond to treatment. The current study was undertaken to investigate mechanisms underlying the failure of PD-1–targeted therapies in patients with advanced renal cell carcinoma (RCC) whose tumors express PD-L1. Formalin-fixed, paraffin-embedded pretreatment tumor biopsies expressing PD-L1 were derived from 13 RCC patients. RNA was isolated from PD-L1$^+$ regions and subjected to whole genome microarray and multiplex quantitative (q)RT-PCR gene expression analysis. A balance between gene expression profiles reflecting metabolic pathways and immune functions was associated with clinical outcomes following anti–PD-1 therapy. In particular, the expression of genes involved in metabolic and solute transport functions such as *UGT1A* family members, also found in kidney cancer cell lines, was associated with treatment failure in patients with PD-L1$^+$ RCC. Conversely, tumors from responding patients overexpressed immune markers such as *BACH2*, a regulator of CD4$^+$ T-cell differentiation, and *CCL3* involved in leukocyte migration. These findings suggest that tumor cell–intrinsic metabolic factors may contribute to treatment resistance in RCC, thus serving as predictive markers for treatment outcomes and potential new targets for combination therapy regimens with anti–PD-1.

Cancer Immunol Res; 4(9); 726–33. ©2016 AACR.

See related Spotlight by Ohashi, p. 719.

Introduction

In renal cell carcinoma (RCC) and some other tumor types, mAbs blocking the programmed death 1 (PD-1):PD-1 ligand (PD-L1, B7-H1) interaction, by targeting either PD-1 (e.g., nivolumab, pembrolizumab) or PD-L1 (e.g., MPDL3280A/atezolizumab, MEDI4736/durvalumab), can induce tumor regression (1–5). Approximately 15% to 30% of patients with advanced RCC experience durable objective tumor regressions following PD-1 pathway blockade (6–9). Attention is now focused on identifying biomarkers predicting response or resistance to anti–PD-1 treatment (10). We previously identified PD-L1 expression on the tumor cell surface as one factor associated with the clinical activity of nivolumab anti–PD-1 in solid tumors including RCC (1). This observation was supported by a subsequent study of nivolumab in RCC, showing a higher objective response rate and prolonged progression-free and overall survival in patients whose pretreatment tumor specimens were PD-L1$^+$ (7), although this finding was not substantiated in a subsequent phase III trial of nivolumab (8). PD-L1 expression by tumor-infiltrating immune cells has been associated with an increased response rate and overall survival following atezolizumab anti–PD-L1 therapy in a nonrandomized trial in RCC (9).

Notably, a significant number of patients with PD-L1$^+$ RCC do not respond to PD-1 pathway blockade, suggesting that additional intratumoral factors may influence treatment outcomes. The current study was undertaken to explore gene expression profiles characterizing PD-L1$^+$ RCCs that did or did not respond to nivolumab anti–PD-1 therapy.

Materials and Methods

Detailed information is available online in Supplementary Materials and Methods.

[1]Department of Oncology, The Johns Hopkins University School of Medicine and Sidney Kimmel Comprehensive Cancer Center, Baltimore, Maryland. [2]Department of Surgery, The Johns Hopkins University School of Medicine and Sidney Kimmel Comprehensive Cancer Center, Baltimore, Maryland. [3]The Lowe Family Genomics Core, The Johns Hopkins University School of Medicine and Sidney Kimmel Comprehensive Cancer Center, Baltimore, Maryland. [4]Oncology Bioinformatics Core, The Johns Hopkins University School of Medicine and Sidney Kimmel Comprehensive Cancer Center, Baltimore, Maryland. [5]Department of Pathology, The Johns Hopkins University School of Medicine and Sidney Kimmel Comprehensive Cancer Center, Baltimore, Maryland. [6]The James Buchanan Brady Urological Institute, The Johns Hopkins University School of Medicine and Sidney Kimmel Comprehensive Cancer Center, Baltimore, Maryland. [7]Department of Dermatology, The Johns Hopkins University School of Medicine and Sidney Kimmel Comprehensive Cancer Center, Baltimore, Maryland.

Note: Supplementary data for this article are available at Cancer Immunology Research Online (http://cancerimmunolres.aacrjournals.org/).

Corresponding Author: Suzanne L. Topalian, Johns Hopkins University School of Medicine, 1550 Orleans Street, CRB2, Room 508, Baltimore, MD 21287. Phone: 410-502-8218, Fax: 410-502-1958; E-mail: stopali1@jhmi.edu

doi: 10.1158/2326-6066.CIR-16-0072

Tumor specimens

Consenting patients with unresectable metastatic RCC received nivolumab anti–PD-1 monotherapy at the Johns Hopkins Kimmel Cancer Center (Baltimore, MD) on one of four clinical trials (NCT00441337, NCT00730639, NCT01354431, NCT01358721) approved by the Johns Hopkins Institutional Review Board. Patients were classified as responders (R) or nonresponders (NR) to anti–PD-1 therapy based on radiographic staging according to Response Evaluation Criteria in Solid Tumors (RECIST; ref. 11). Pretreatment tumor specimens were characterized for PD-L1 expression by IHC as described previously (refs. 1, 12; Supplementary Table S1).

Immunohistochemical analysis

Serial 5-μm-thick sections from PD-L1$^+$ formalin-fixed, paraffin-embedded (FFPE) tumor specimens were stained for the expression of selected markers with specific mAbs as described previously (13). PD-L1$^+$ tumor specimens had $\geq$5% of tumor cells showing cell surface staining with the murine anti-human PD-L1 mAb 5H1 (from Lieping Chen, Yale University, New Haven, CT). Comparisons of IHC results from PD-L1$^+$ tumors derived from responding versus nonresponding patients were performed using The R Project for Statistical Computing (https://www.r-project.org/).

Multiplex quantitative (q)RT-PCR assays and statistical analysis

PD-L1$^+$ tumor areas, identified with IHC on neighboring tissue sections, were either manually dissected by scraping with a scalpel, or were laser-capture microdissected from 5-μm FFPE tissue sections as described previously (refs. 12, 14; Supplementary Fig. S1). Total RNA was isolated from PD-L1$^+$ tumor areas and the expression of selected genes was quantified using custom-made TaqMan Low-Density Array Micro Fluidic Cards per protocol (TLDA; Applied Biosystems), as described previously (14).

Whole genome expression profiling and analysis

Global gene expression in pretreatment RCC specimens was measured by DASL (cDNA-mediated annealing, selection, extension, and ligation) assays arrayed on the Illumina Human HT-12 WG-DASL V4.0 R2 expression BeadChip, as per the manufacturer's specifications (Illumina) as previously described (14). Gene expression data are accessible through GEO Series accession number GSE67501 (http://www.ncbi.nlm.nih.gov/geo/query/acc.cgi?acc=GSE67501).

RCC cell lines

Eight RCC cell lines (786-0, A498, ACHN, Caki I, RXF-393, TK-10, SN12C, and U0-31) from the NCI-60 panel were obtained in 2009 from the NCI-Frederick Cancer Center DCTD Tumor/Cell Repository (Frederick, MD). Characterization is provided at https://dtp.cancer.gov/discovery_development/nci-60/characterization.htm. They were cryopreserved and used within 6 months of continuous culture. RCC cell lines were assessed with multiplex qRT-PCR for selected gene expression.

Cytotoxicity assays

The established melanoma cell lines 397-mel and 888-mel, generated from metastatic melanoma lesions in our laboratory and maintained as described previously (15, 16) were transfected with the empty vector pCMV6-Entry or with pCMV6-UGT1A6 encoding human UGT1A6 (RC215957; Origene Technologies) using Lipofectamine 2000 (Life Technologies). qRT-PCR and Western blotting revealed no UGT1A6 in these melanomas prior to transfection, and positive expression after transfection with the plasmid encoding UGT1A6, but not with the control vector. Tumor cell lysis was measured with a modified flow cytometry–based assay detecting the disappearance of CFSE-labeled transfectants expressing UGT1A6 or not, upon incubation with nonspecific LAK cells or specific T effector cells (17).

In silico correlation of *UGT1A6* expression with overall survival in RCC

RNA sequencing data from The Cancer Genome Atlas project (TCGA), including 444 clear cell RCC samples and 72 matched normal kidney samples, were used for *in silico* analysis (18). Data were analyzed using R/Bioconductor software.

Results

Immune-related genes overexpressed in PD-L1$^+$ melanomas are uniformly expressed in PD-L1$^+$ RCCs regardless of anti–PD-1 treatment outcome

In a prior study of archival melanoma specimens, we identified immune-related genes that were coordinately overexpressed in PD-L1$^+$ compared with PD-L1$^-$ tumors (14). They included genes associated with CD8$^+$ T-cell activation (*CD8A*, *IFNG*, *PRF1*, *CCL5*), antigen presentation (*CD163*, *TLR3*, *CXCL1*, *LYZ*), and immunosuppression [*PD1*, *CD274* (PD-L1), *LAG3*, *IL10*]. In the current study, multiplex qRT-PCR was used to characterize pretreatment PD-L1$^+$ RCC specimens from 12 patients receiving anti–PD-1 (R = 4, NR = 8) for immune markers (Supplementary Table S1). Genes that were coordinately overexpressed in PD-L1$^+$ melanomas were also expressed in PD-L1$^+$ RCCs. However, none were significantly differentially expressed according to clinical outcomes after nivolumab therapy (data not shown). Similar results were obtained when IHC was used to examine protein expression for a more focused group of immune-related molecules in RCCs from 13 patients (R = 4, NR = 9), including PD-1, PD-L2, LAG-3, and TIM-3, and to characterize infiltrating immune cell subsets (FoxP3, CD4:CD8 ratio; Supplementary Fig. S2). No significant differences in expression of these molecules were observed between PD-L1$^+$ RCCs from responders versus nonresponders. Thus, all PD-L1$^+$ RCCs appeared to have an immune-reactive tumor microenvironment (TME) which, in itself, did not distinguish responders from nonresponders.

Increased intratumoral expression of genes with metabolic functions is associated with resistance of PD-L1$^+$ RCCs to anti–PD-1 therapy

Because analysis of a selected panel of 60 immune-related genes did not reveal significant differences between PD-L1$^+$ RCCs that were responsive or resistant to anti–PD-1 therapy, we next turned to whole genome expression profiling. Eleven available RCC specimens from among the original cohort (R = 4, NR = 7; Supplementary Table S1) were analyzed for the expression of 29,377 gene targets. We identified 234 probes corresponding to 223 genes that were differentially expressed between the two groups, based on a P of $\leq$ 0.01 and expression fold change magnitude $\geq$1.5. Among them, 116 probes corresponding to 113 genes were upregulated in tumors from responding patients, and 118 probes corresponding to 110 genes were upregulated in tumors from nonresponding patients (Fig. 1A; Supplementary

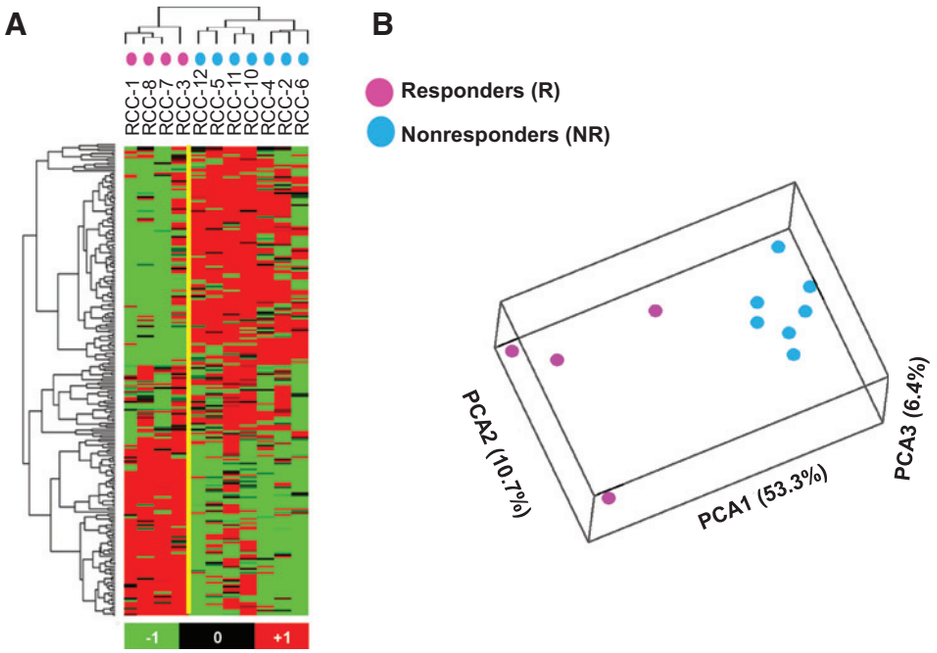

Figure 1.
Whole genome microarray analysis of pretreatment PD-L1$^+$ RCC specimens shows differential gene expression between patients responding or not to anti–PD-1 therapy. **A,** heatmap and cluster analysis based on differentially expressed genes detected by 234 Illumina probes satisfying the criteria of Student *t* test $P \leq 0.01$ and fold change magnitude ≥ 1.5, comparing tumors from responders (R, $n = 4$) versus nonresponders (NR, $n = 7$). Data were analyzed with BRBArray Tools (http://linus.nci.nih.gov/BRB-ArrayTools.html) and visualized by Stanford Cluster Program and TreeView software. Red, high gene expression; green, low gene expression. **B,** principal component analysis (PCA) based on 1,017 Illumina probes having differential expression in tumors from responding (R) versus nonresponding (NR) patients, with $P \leq 0.05$ and fold change magnitude ≥ 1.5. Separation of the R and NR samples is seen. The principal component axis directions are labeled, with the percentage of the total variance captured by each axis in parentheses.

Table S2). By inspection, genes upregulated in nonresponders appeared to be functionally related in metabolic pathways. In contrast, some genes that were upregulated in tumors from responding patients had immune functions. Thus, there appeared to be a functional dichotomy of gene expression profiles in PD-L1$^+$ RCCs obtained from patients who responded or did not respond to anti–PD-1 therapy. To further explore these trends, a functional annotation analysis was performed with the DAVID Bioinformatics Resources 6.7 tool, based on 1,017 Illumina probes having differential expression in tumors from responding versus nonresponding patients with fold expression change ≥ 1.5 and $P \leq 0.05$. A principal component analysis (PCA; ref. 19) of the entire set of 1,017 probes further revealed the segregation of gene expression profiles in RCCs from responding versus nonresponding patients (Fig. 1B). Among the 1,017 probes, 467 and 550 were found to be overexpressed in responders and nonresponders, respectively. Analysis of the 467 probes that were overexpressed in responders did not yield significant DAVID gene clusters. However, analysis of the 550 probes that were overexpressed in nonresponders yielded 23 pathways involving mitochondrial and other metabolic functions (DAVID Benjamini FDR ≤ 0.010; Table 1).

Investigation of differentially expressed genes with multiplex qRT-PCR

To further explore the results of global gene expression profiling, differential expression of 60 selected unique gene targets was assessed with multiplex qRT-PCR in 12 specimens (R = 4, NR = 8; Supplementary Table S3). By considering results obtained with each of four endogenous gene controls, 25 among the 60 queried genes were confirmed to be differentially expressed in the two groups of patients with divergent clinical outcomes (Table 2). These 25 genes were not differentially expressed in RCC specimens from primary versus metastatic sites (not shown). In particular, upregulation of genes corresponding to proteins associated with metabolic and solute transport functions was found in nonresponders (Fig. 2A). These proteins are known to have physiologic functions in normal renal epithelial cells. Among them, the UDP-glucuronosyltransferase *UGT1A6* showed the greatest differential expression, being upregulated approximately 300-fold in nonresponders ($P = 0.007$ using *GUSB* endogenous control). Its family members *UGT1A1* and *UGT1A3* were also overexpressed in nonresponders. In addition, genes encoding proteins involved in solute transport, such as the potassium channel rectifier *KCNJ16*, the glucose-6-phosphate translocase *SLC37A4*, the human sodium-dependent ascorbic acid (vitamin C) transporter *SLC23A1*, and the myelin and lymphocyte–associated protein *MAL*, were also significantly upregulated in RCCs from nonresponding patients. In contrast, some genes associated with immune functions were upregulated in tumors from responding patients, including the chemokine *CCL3*, the plectin molecule (*PLEC*), the nuclear factor *NFATC1*, the transcription regulator *BACH2*, and the histone methyltransferase *WHSC1* (Fig. 2A). Thus, qRT-PCR confirmed the dichotomous pattern of gene expression suggested by whole genome

Table 1. Functionally annotated gene categories from DAVID analysis of whole genome microarray results, comparing RCCs from responders to nonresponders

Functionally related group of genes[a]	Number of genes in submitted list/total number of genes in the category (%)	P[b]	Benjamini multiple comparison adjusted P
GO: mitochondrion	72/1,087 (6.6)	6.20E−13	2.32E−10
Swiss-Prot: mitochondrion	57/832 (6.9)	1.02E−11	4.02E−09
GO: coenzyme binding	24/181 (13.3)	1.19E−10	7.55E−08
GO: mitochondrial part	45/595 (7.6)	6.51E−10	1.22E−07
Swiss-Prot: oxidoreductase	42/562 (7.5)	6.89E−10	1.35E−07
GO: oxidation reduction	47/639 (7.4)	8.04E−11	1.62E−07
GO: cofactor binding	26/249 (10.4)	2.86E−09	9.08E−07
GO: organelle membrane	63/1,096 (5.7)	7.99E−09	9.96E−07
GO: mitochondrial envelope	34/419 (8.1)	2.35E−08	2.19E−06
Swiss-Prot: transit peptide	34/476 (7.1)	1.13E−07	1.11E−05
GO: mitochondrial membrane	29/394 (7.4)	2.25E−06	1.69E−04
GO: envelope	38/622 (6.1)	3.75E−06	2.00E−04
GO: organelle envelope	38/620 (6.1)	3.45E−06	2.15E−04
Swiss-Prot: endoplasmic reticulum	40/713 (5.6)	3.36E−06	2.64E−04
UniProt: transit peptide: mitochondrion	33/467 (7.1)	2.62E−07	3.06E−04
Swiss-Prot: nad	18/189 (9.5)	4.96E−06	3.25E−04
GO: mitochondrial inner membrane	22/306 (7.2)	7.10E−05	0.00265
GO: organelle inner membrane	23/329 (7.0)	7.05E−05	0.00292
GO: endoplasmic reticulum	47/960 (4.9)	6.68E−05	0.00312
Swiss-Prot: mitochondrion inner membrane	16/193 (8.3)	9.65E−05	0.00540
GO: acyl-CoA binding	6/16 (37.5)	3.17E−05	0.00670
GO: monovalent inorganic cation transmembrane transporter activity	12/104 (11.5)	5.26E−05	0.00833
GO: hydrogen ion transmembrane transporter activity	11/90 (12.2)	7.56E−05	0.00957

NOTE: Shown are functional gene categories upregulated in tumors from nonresponders and having a Benjamini adjusted P value (FDR) from DAVID of $\leq$0.010. The list submitted to DAVID contained 550 Illumina probe IDs for which the nonresponder/responder expression level fold change was $\geq$ 1.5 and the equal variance two-sided t test P value was $\leq$0.05. Gene groups are ordered according to the Benjamini adjusted P values.

[a]Nomenclature as per DAVID web tool (https://david.ncifcrf.gov/).

[b]DAVID adjustment of the Fisher exact test (hypergeometric distribution) P value.

microarray in tumors from responding versus nonresponding patients.

Genes upregulated in PD-L1$^+$ RCCs resistant to anti–PD-1 therapy are also expressed by kidney cancer cell lines

The RCC TME is a complex milieu containing many different cell types. To understand whether metabolic genes that were overexpressed in tumor specimens from nonresponding patients were specifically associated with renal carcinoma cells, we evaluated their expression in 8 established kidney cancer cell lines using qRT-PCR. Results showed that cultured renal carcinoma cells expressed the metabolic genes of interest (Supplementary Fig. S3).

UGT1A6 protein is overexpressed in PD-L1$^+$ RCCs associated with nonresponse to anti–PD-1 therapy

UGT1A6 is involved in the chemical "defensome" and detoxifies exogenous and stress-related lipids (20). In whole genome expression profiling and qRT-PCR assessment, it was the most highly overexpressed gene associated with nonresponse to anti–PD-1 ($\sim$8-fold and $\sim$300-fold, $P \leq 0.005$ with multiple probes and $P = 0.007$, respectively). Therefore, the expression of UGT1A6 in RCC was further explored at the protein level with IHC in the same 12 specimens as those used for gene expression profiling by qRT-PCR. UGT1A6 protein expression varied widely among the specimens and was associated with clinical outcomes following anti–PD-1 therapy ($P = 0.036$, one-sided Wilcoxon rank-sum test; Fig. 2B).

Melanoma cells transfected with *UGT1A6* are not resistant to lysis by immune cells *in vitro*

To examine whether overexpression of UGT1A6 protein might protect tumor cells from immune cell killing, we tested the ability of non-MHC–restricted LAK cells and MHC I–restricted T cells (397 TILs or 888 TILs) to lyse 397-mel or 888-mel cells transfected with a plasmid encoding *UGT1A6*. No substantial difference in lysis of UGT1A6-positive or -negative melanoma cells was observed (not shown).

Expression of *UGT1A6* is not associated with survival in patients with RCC

To explore whether the observed overexpression of genes such as *UGT1A6* is specifically associated with adverse outcomes to anti–PD-1 therapy, or generally associated with poor prognosis in patients with RCC, an *in silico* analysis was performed on RNA expression data obtained from 444 primary clear cell RCC specimens in The Cancer Genome Atlas project (TCGA; ref. 18). Kaplan–Meier curves were generated using the median expression value for *UGT1A6* to segregate samples into high or low expressers. There was no significant correlation between the level of *UGT1A6* mRNA expression in primary kidney cancers and overall survival in the entire cohort of 444 patients, nor with survival in a subset of 71 patients with stage IV metastatic disease (similar to patients in our study; Supplementary Fig. S4A). Furthermore, *UGT1A6* expression levels did not correlate with RCC clinical stage in an analysis of TCGA data (Supplementary Fig. S4B). These findings suggest that the association of *UGT1A6* expression with clinical outcomes following anti–PD-1 therapy is specifically relevant in the context of this treatment.

Discussion

Expression of the immunosuppressive ligand PD-L1, detected in pretreatment tumor biopsies with IHC, has been associated

Table 2. Genes differentially expressed in RCCs from responding versus nonresponding patients, assessed by qRT-PCR

		GUSB		PTPRC	
Gene symbol[a]	**Protein function[b]**	**FC R/NR**	***P*[c]**	**FC R/NR**	***P*[c]**
AKR1C3	Aldo-keto reductase family member, which catalyzes the conversion of aldehydes and ketones to alcohols and the reduction of prostaglandin D2 and phenanthrenequinone.	−5.6	0.015	−6.1	0.015
BACH2	Transcription regulator, which induces apoptosis in response to oxidative stress and represses effector programs to stabilize Treg-mediated immune homeostasis.	3.2	0.027	2.9	0.150
BMP1	Bone morphogenetic protein 1, which cleaves the C-terminal propeptides of procollagen I, II, and III and induces cartilage and bone formation.	3.6	0.012	3.3	0.137
CACNB1	Voltage-dependent L-type calcium channel subunit beta-1, which contributes to the function of the calcium channel by increasing peak calcium current.	4.8	0.009	4.4	0.017
CCL3	C-C motif chemokine 3 with inflammatory and chemokinetic properties.	3.5	0.038	3.2	0.071
CD24	Signal transducer CD24, which modulates B-cell activation responses.	−7.0	0.051	−7.7	0.048
E2F8	Transcription factor E2F8, which participates in various processes such as angiogenesis and polyploidization of specialized cells.	2.6	0.001	2.4	0.071
ENPP5	Ectonucleotide pyrophosphatase/phosphodiesterase family member, which may play a role in neuronal cell communication.	−5.4	0.013	−5.9	0.054
F2RL1	Proteinase-activated receptor, which mediates inhibition of tumor necrosis factor alpha (TNF).	−26.3	0.047	−28.9	0.047
IL11RA	Receptor for interleukin-11, which might be involved in the control of proliferation and/or differentiation of skeletogenic progenitor or other mesenchymal cells.	3.0	0.013	2.8	0.097
KCNJ16	Inward rectifier potassium channel, which mediates regulation of fluid and pH balance.	−13.2	0.010	−14.5	0.018
LTBP1	Latent-transforming growth factor beta-binding protein, which may play critical roles in controlling the activity of transforming growth factor beta 1 (TGFB) and may have a structural role in the extracellular matrix.	2.0	0.009	1.8	0.230
MAL	Myelin and lymphocyte protein, which can be an important component in the vesicular trafficking between the Golgi complex and the apical plasma membrane.	−20.6	0.020	−22.6	0.016
MYLK2	Myosin light chain kinase, implicated in the level of global muscle contraction and cardiac function.	53.4	0.050	48.6	0.072
NFATC1	Nuclear factor of activated T-cells, which plays a role in the inducible expression of cytokine genes in T cells regulating their activation and proliferation but also their differentiation and programmed death.	3.3	0.003	3.0	0.055
PITX2	Pituitary homeobox, which controls cell proliferation in a tissue-specific manner and is involved in morphogenesis.	22.4	0.095	20.3	0.075
PLEC	Plectin, which interlinks intermediate filaments with microtubules and microfilaments and anchors intermediate filaments to desmosomes.	2.6	0.020	2.4	0.246
SLC23A1	Solute carrier member, which mediates electrogenic uptake of vitamin C.	−16.6	0.066	−18.2	0.091
SLC37A4	Glucose-6-phosphate translocase, which plays a central role in homeostatic regulation of glucose.	−2.3	0.081	−2.3	0.239
TNFRSF19	Tumor necrosis factor receptor family member, which mediates activation of Jun N-terminal kinase (JNK) and nuclear factor-kappa-B (NF-κB), possible promoting caspase-independent cell death.	7.1	0.011	6.4	0.112
UCP3	Mitochondrial uncoupling protein 3, involved in mitochondrial transport uncoupling oxidative phosphorylation.	4.8	0.001	4.4	0.051
UGT1A1	UDP-glucuronosyltransferases, which mediate the elimination of toxic xenobiotics and endogenous compounds.	−7.1	0.028	−7.8	0.098
UGT1A3		−5.0	0.062	−5.5	0.110
UGT1A6		−287.7	0.007	−316.1	0.012
WHSC1	Histone-lysine N-methyltransferase, which acts as a transcription regulator of cytokines.	2.3	0.006	2.1	0.293

NOTE: Listed are genes with expression fold change magnitude (FC) ≥ 2 and $P \leq 0.1$ (Student *t* test) when normalized to either *GUSB* or *PTPRC* (CD45) expression. Positive FC indicates genes overexpressed in tumors from responding (R) patients; negative FC indicates overexpression in tumors from nonresponding (NR) patients.

[a]Refers to the official gene name (http://www.ncbi.nlm.nih.gov/gene/).

[b]Obtained from HUGO Gene Nomenclature Committee website: http://www.genenames.org/.

[c]Data were analyzed using the comparative C_t method ($\Delta\Delta C_t$), normalized to either *GUSB* (beta-glucuronidase) or *PTPRC* (CD45, pan immune cell marker). A two-tailed, unpaired Student *t* test was used to determine the statistical significance of FC values.

with favorable clinical outcomes following PD-1– and PD-L1–blocking therapies in some studies in several types of cancer (1, 7, 9, 21). This can be understood by viewing PD-L1 as a surrogate marker for an immune-reactive TME, as inflammatory cytokines such as IFNγ are major drivers of PD-L1 expression on tumor and stromal cells. In this model, blocking the PD-1/PD-L1 interaction unleashes an immune response that is already properly trained and poised to attack cancer cells, but held in check by this immunosuppressive pathway. Despite the therapeutic impact of PD-1 blockade in many patients with certain cancer

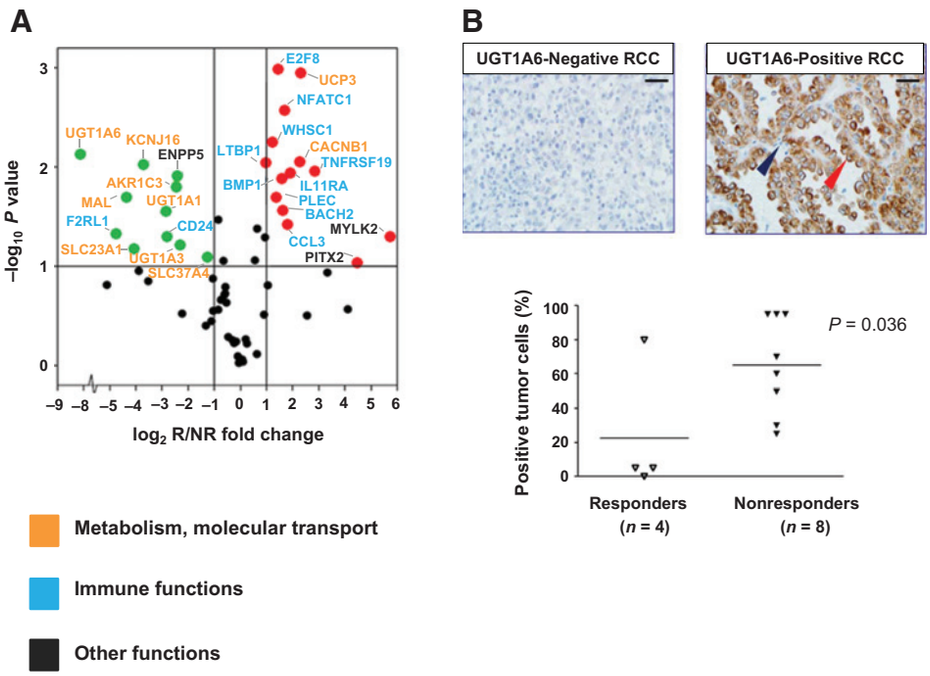

Figure 2.

Genes overexpressed in pretreatment PD-L1$^+$ RCC specimens from responding versus nonresponding patients reflect immune versus metabolic functions, respectively. **A,** results of multiplex qRT-PCR for 60 select genes are shown, amplifying RNA isolated from pretreatment tumors in 4 responders and 8 nonresponders. Red and green dots represent genes significantly overexpressed or underexpressed, respectively, by at least 2-fold in tumors from responders compared with nonresponders, and with a two-sided $P \leq 0.1$ (indicated by the horizontal line). Gene names are color coded according to biological functions. The *GUSB* transcript was used as the internal reference. *UGT1A6* was the most highly overexpressed gene associated with nonresponse to anti–PD-1. Similar results were obtained using *18S*, *ACTB*, or *PTPRC* (CD45) as reference genes. Supporting information is provided in Table 2 and Supplementary Table S3. **B,** UGT1A6 protein expression was evaluated by IHC in the same 12 pretreatment PD-L1$^+$ RCC specimens as were studied with qRT-PCR, including tumors from 4 responders and 8 nonresponders. Top, representative UGT1A6 negative (left) and positive (right) RCC specimens are shown. Scale bars, 25 μm. Red arrow, kidney cancer cell with positive staining; blue arrow, infiltrating lymphocyte devoid of staining. Bottom, UGT1A6 expression is quantified by percent positive tumor cells in each specimen. Horizontal black bars indicate mean values. Enhanced UGT1A6 expression was significantly associated with nonresponse to anti–PD-1 therapy ($P = 0.036$, one-sided Wilcoxon rank-sum test).

types (22), the majority of patients with PD-L1$^+$ tumors do not respond to anti–PD-1/PD-L1 drugs, suggesting the involvement of additional factors in the TME contributing to treatment resistance. The current study attempts to identify such factors by exploring the gene expression landscape of PD-L1$^+$ RCCs derived from patients with divergent clinical outcomes after anti–PD-1 therapy, and identifies groups of metabolic and immunologic factors associated with adverse or favorable clinical outcomes, respectively.

RCC has been characterized as a metabolic disease, with the signature upregulation of factors adapting to hypoxia and functioning to meet the bioenergetic demands of cellular proliferation (23). We here describe a likely metabolic shift in RCCs resistant to anti–PD-1 therapy, with overexpression of molecules associated with glucuronidation and the transport of solutes and nutrients such as glucose. Among them, UGT1A6, whose principal role is to promote cellular clearance of toxins and exogenous lipophilic chemicals (18), was the single most highly overexpressed molecule associated with anti–PD-1 treatment resistance, and other UGT1A family members and solute carriers constituting the chemical "defensome" were also upregulated. This gene expression profile may simply reflect an activated cell phenotype; however, one might hypothesize that the heightened clearance of toxins from tumor cells by molecules typified by UGT1A6 may render them more fit to outpace the immune system. Furthermore, the overexpression of metabolic genes in RCCs resistant to anti–PD-1 therapy may reflect tumor-imposed metabolic effects that can restrict the responsiveness of tumor-specific infiltrating T cells by competing for vital nutrients such as glucose within the TME (24).

Despite the limitations inherent to this retrospective study of a small number of specimens, the significantly differential gene expression profiles described here provide a basis for future exploration in larger RCC cohorts, potentially including PD-L1$^+$ and (−) tumors. The general approach to identifying biomarkers of clinical response to PD-1–targeted therapies has so far focused on immunologic factors in the TME. However, a deeper level of investigation may be warranted for individual tumor types, and intersections of tumor cell–intrinsic factors with immunologic factors may be particularly revealing. For instance, a recent study unexpectedly found overexpression of β-catenin to be associated with decreased infiltration of tumor-specific T cells in melanoma (25). A greater knowledge of such tumor-intrinsic mechanistic markers may reveal new therapeutic targets for combination treatment regimens based on PD-1 pathway blockade, and useful markers for selecting patients most likely to respond to these therapies.

Disclosure of Potential Conflicts of Interest

R.A. Anders reports receiving commercial research support from Five Prime Diagnostics and Bristol-Myers Squibb and is a consultant/advisory board member for Adapative Biotech. C.G. Drake reports receiving commercial research support from Bristol-Myers Squibb, Janssen, and Aduro Biotech; has ownership interest (including patents) in Potenza and Compugen; and is a consultant/advisory board member for Compugen, Dendreon, Roche/Genentech, Merck, Eli Lilly, and AstraZeneca/Medimmune. D.M. Pardoll reports receiving commercial research support and has an ownership interest (including patents) in Bristol-Myers Squibb. J.M. Taube reports receiving commercial research support from Bristol-Myers Squibb and is a consultant/advisory board member for Bristol-Myers Squibb, Merck, and AstraZeneca. S.L. Topalian has served as a consultant/advisory board member for Five Prime Therapeutics, MedImmune, Merck, and Pfizer, and has an ownership interest in Bristol-Myers Squibb, Potenza Therapeutics, and Five Prime Therapeutics. No potential conflicts of interest were disclosed by the other authors.

Authors' Contributions

Conception and design: R.A. Anders, J.M. Taube, S.L. Topalian
Development of methodology: M.L. Ascierto, H. Xu, J. Fan, J.M. Taube, S.L. Topalian
Acquisition of data (provided animals, acquired and managed patients, provided facilities, etc.): T.L. McMiller, R.A. Anders, G.J. Netto, C. Cheadle, J.M. Taube
Analysis and interpretation of data (e.g., statistical analysis, biostatistics, computational analysis): M.L. Ascierto, A.E. Berger, L. Danilova, R.A. Anders, T.S. Pritchard, L. Cope, C.G. Drake, J.M. Taube, S.L. Topalian
Writing, review, and/or revision of the manuscript: M.L. Ascierto, T.L. McMiller, A.E. Berger, L. Danilova, G.J. Netto, T.S. Pritchard, L. Cope, C.G. Drake, D.M. Pardoll, J.M. Taube, S.L. Topalian
Administrative, technical, or material support (i.e., reporting or organizing data, constructing databases): M.L. Ascierto
Study supervision: S.L. Topalian
Other (developed the IHC protocol and performed relevant IHC staining): H. Xu

Acknowledgments

The authors would like to thank Dr. Hans Hammers, Dr. Jenny Kim, Ting Wang and Yelena Millman (Johns Hopkins University) for providing clinical response data; Dr. Lieping Chen (Yale University) for providing the anti–PD-L1 mAb 5H1; Dr. Shuming Chen, George A. Crabill, and Matthew Presby (Johns Hopkins University) for helpful discussions and technical assistance; Jessica Esandrio for administrative assistance; and Dr. Mark Ratain (University of Chicago) and Dr. David Feltquate (Bristol-Myers Squibb) for helpful discussions.

Grant Support

This study was supported by research grants from Bristol-Myers Squibb (to S.L. Topalian); the National Cancer Institute, NIH (R01 CA142779; to J. M. Taube, D.M. Pardoll, and S.L. Topalian; and P30 CA0006973, all authors); the Bloomberg~Kimmel Institute for Cancer Immunotherapy at Johns Hopkins (to R.A. Anders, C.G. Drake, D.M. Pardoll, J.M. Taube, and S.L Topalian); and Stand Up To Cancer—Cancer Research Institute Cancer Immunology Translational Cancer Research Grant SU2C-AACR-DT1012 (to R.A. Anders, J.M. Taube, D.M. Pardoll, and S.L. Topalian). Stand Up To Cancer is a program of the Entertainment Industry Foundation administered by the American Association for Cancer Research.

The costs of publication of this article were defrayed in part by the payment of page charges. This article must therefore be hereby marked *advertisement* in accordance with 18 U.S.C. Section 1734 solely to indicate this fact.

Received May 4, 2016; revised June 23, 2016; accepted June 24, 2016; published OnlineFirst August 4, 2016.

References

1. Topalian SL, Hodi FS, Brahmer JR, Gettinger SN, Smith DC, McDermott DF, et al. Safety, activity, and immune correlates of anti-PD-1 antibody in cancer. N Engl J Med 2012;366:2443–54.
2. Brahmer JR, Tykodi SS, Chow LQ, Hwu WJ, Topalian SL, Hwu P, et al. Safety and activity of anti-PD-L1 antibody in patients with advanced cancer. N Engl J Med 2012;366:2455–65.
3. Brahmer JR, Drake CG, Wollner I, Powderly JD, Picus J, Sharfman WH, et al. Phase I study of single-agent anti-programmed death-1 (MDX-1106) in refractory solid tumors: safety, clinical activity, pharmacodynamics, and immunologic correlates. J Clin Oncol 2010;28:3167–75.
4. Hamid O, Robert C, Daud A, Hodi FS, Hwu WJ, Kefford R, et al. Safety and tumor responses with lambrolizumab (anti-PD-1) in melanoma. N Engl J Med 2013;369:134–44.
5. Nghiem PT, Bhatia S, Lipson EJ, Kudchadkar RR, Miller NJ, Annamalai L, et al. PD-1 Blockade with pembrolizumab in advanced Merkel-cell carcinoma. N Engl J Med 2016;374:2542–52.
6. McDermott DF, Drake CG, Sznol M, Choueiri TK, Powderly JD, Smith DC, et al. Survival, durable response, and long-term safety in patients with previously treated advanced renal cell carcinoma receiving nivolumab. J Clin Oncol 2015;33:2013–20.
7. Motzer RJ, Rini BI, McDermott DF, Redman BG, Kuzel TM, Harrison MR, et al. Nivolumab for metastatic renal cell carcinoma: results of a randomized phase II trial. J Clin Oncol 2015;33:1430–7.
8. Motzer RJ, Escudier B, McDermott DF, George S, Hammers HJ, Srinivas S, et al. Nivolumab versus everolimus in advanced renal-cell carcinoma. N Engl J Med 2015;373:1803–13.
9. McDermott DF, Sosman JA, Sznol M, Massard C, Gordon MS, Hamid O, et al. Atezolizumab, an anti-programmed death-ligand 1 antibody, in metastatic renal cell carcinoma: long-term safety, clinical activity, and immune correlates from a phase Ia study. J Clin Oncol 2016;34:833–42
10. Topalian SL, Taube JM, Anders RA, Pardoll DM. Mechanism-driven biomarkers to guide immune checkpoint blockade in cancer therapy. Nat Rev Cancer 2016;16:275–87.
11. Therasse P, Arbuck SG, Eisenhauer EA, Wanders J, Kaplan RS, Rubinstein L, et al. New guidelines to evaluate the response to treatment in solid tumors. European Organization for Research and Treatment of Cancer, National Cancer Institute of the United States, National Cancer Institute of Canada. J Nat Cancer Inst 2000;92:205–16.
12. Taube JM, Anders RA, Young GD, Xu H, Sharma R, McMiller TL, et al. Colocalization of inflammatory response with B7-h1 expression in human melanocytic lesions supports an adaptive resistance mechanism of immune escape. Sci Transl Med 2012;4:127ra37.
13. Taube JM, Klein A, Brahmer JR, Xu H, Pan X, Kim JH, et al. Association of PD-1, PD-1 ligands, and other features of the tumor immune microenvironment with response to anti-PD-1 therapy. Clin Cancer Res 2014;20:5064–74.
14. Taube JM, Young GD, McMiller TL, Chen SM, Salas JT, Pritchard TS, et al. Differential expression of immune-regulatory genes associated with PD-L1 display in melanoma: implications for PD-1 pathway blockade. Clin Cancer Res 2015;21:3969–76.
15. Topalian SL, Solomon D, Rosenberg SA. Tumor-specific cytolysis by lymphocytes infiltrating human melanomas. J Immunol 1989;142:3714–25.
16. Robbins PF, El-Gamil M, Kawakami Y, Stevens E, Yannelli JR, Rosenberg SA. Recognition of tyrosinase by tumor-infiltrating lymphocytes from a patient responding to immunotherapy. Cancer Res 1994;54:3124–6.
17. Purwar R, Schlapbach C, Xiao S, Kang HS, Elyaman W, Jiang X, et al. Robust tumor immunity to melanoma mediated by interleukin-9-producing T cells. Nat Med 2012;18:1248–53.
18. The Cancer Genome Atlas Research Network. Comprehensive molecular characterization of clear cell renal cell carcinoma. Nature 2013;499:43–9.

19. Jolliffe IT. Principal component analysis, second edition. New York, NY: Springer-Verlag New York, Inc; 2002.
20. Wells PG, Mackenzie PI, Chowdhury JR, Guillemette C, Gregory PA, Ishii Y, et al. Glucuronidation and the UDP-glucuronosyltransferases in health and disease. Drug Metab Dispos 2004;32:281–90.
21. Herbst RS, Soria JC, Kowanetz M, Fine GD, Hamid O, Gordon MS, et al. Predictive correlates of response to the anti-PD-L1 antibody MPDL3280A in cancer patients. Nature 2014;515:563–7.
22. Topalian SL, Drake CG, Pardoll DM. Immune checkpoint blockade: a common denominator approach to cancer therapy. Cancer Cell 2015;27:450–61.
23. Linehan WM, Srinivasan R, Schmidt LS. The genetic basis of kidney cancer: a metabolic disease. Nat Rev Urol 2010;7:277–85.
24. Chang CH, Qiu J, O'Sullivan D, Buck MD, Noguchi T, Curtis JD, et al. Metabolic competition in the tumor microenvironment is a driver of cancer progression. Cell 2015;162:1229–41
25. Spranger S, Bao R, Gajewski TF. Melanoma-intrinsic beta-catenin signalling prevents anti-tumour immunity. Nature 2015;523:231–5.